UDK 669.721.5:539.536 ISSN 1580-2949
Original scientific article/Izvirni znanstveni članek MTAEC9, 57(1)63(2023)

EFFECT OF THICKNESS REDUCTIONS ON MICROSTRUCTURE AND NANO-MECHANICAL PROPERTIES OF AZ31 MAGNESIUM ALLOY IN FLOW-FORMING

VPLIV ZMANJŠANJA DEBELINE NA MIKROSTRUKTURO IN NANOMEHANSKE LASTNOSTI MAGNEZIJEVE ZLITINE VRSTE AZ31 MED PLASTIČNIM PREOBLIKOVANJEM

Han Zhang[1], Tingting Zhang[2,3], Jie Zhang[1], Zhihang Yan[1], Wenxian Wang[1,*]

[1]College of Materials Science and Engineering, Taiyuan University of Technology, Taiyuan, China
[2]College of Mechanical and Vehicle Engineering, Taiyuan University of Technology, Taiyuan, China
[3]Engineering Research Center of Advanced Metal Composites Forming Technology and Equipment, Ministry of Education, Taiyuan, China

Prejem rokopisa – received: 2022-10-14; sprejem za objavo – accepted for publication: 2022-12-22

doi:10.17222/mit.2022.659

The effect of reducing the thinning rate when flow forming AZ31B magnesium alloy barrels on the microstructure, crystal orientation, micro-, nano- and macro-mechanical properties was investigated. The results demonstrate that when the magnesium alloy undergoes different degrees of plastic deformation after flow forming, the grain size and dislocation density inside the crystal change greatly, and the evolution pattern of the organization has a significant effect on the mechanical properties of the materials. The stress-strain curve of the cylindrical parts was obtained by nano-indentation and hardness. This is important to improve the mechanical properties of the magnesium alloy.

Keywords: flow forming, microstructure, nanomechanical properties, hardness

V članku je predstavljena raziskava vpliva zmanjšanja hitrosti tanjšanja materiala med plastičnim preoblikovanjem valjčkov iz magnezijeve zlitine vrsteAZ31B na njeno mikrostrukturo, orientacijo kristalov ter njene makro-, mikro- in nanomehanske lastnosti. Rezultati raziskav so pokazali, da se zaradi različnih stopnej deformacije med izbranim protokolom plastičnega preoblikovanja močno spremeni velikost kristalnih zrn in gostota dislokacijizbrane zlitine, kar močno vpliva tudi na njene mehanske lastnosti. Krivulje napetost-deformacija cilindričnih delov so izdelali s pomočjo nano indentacije (vtiskovanja nano prizme) in meritev trdote. Rezultati te raziskave so pomembni s stališča izboljšanja mehanskih lastnosti magnezijevih zlitin.

Ključne besede:plastično preoblikovanje, mikrostruktura, nano-mehanske lastnosti, trdota

1 INTRODUCTION

As lightweight materials, magnesium (Mg) and its alloys are relevant in many areas of the automotive, aerospace and weapons industries.[1–4] Mg alloys usually exhibit poor ductility and plasticity due to their hexagonal-close-packed (hcp) lattice.[5–7] Mg alloys are conventionally formed by casting,[8] rolling,[9] forging[10] and extrusion.[11] Although progress has been made in these areas, these processes are prone to defects such as cracking and flaking, and these factors have severely restricted the application and development of thin-walled magnesium alloy tubes.[12,13]

Flow forming is an effective plastic deformation process to fabricate high-precision, thin-walled cylindrical components by employing an incremental rotary point deformation technique.[14–16] As a chipless metal-forming process, flow forming can reduce the wall thickness of a pre-form or tube without changing the inner diameter, and is an efficient and environmentally friendly metal-forming process. In recent years, flow forming has been widely utilized in the production of modern industrial products, such as flanged components and seamless tubes, for high precision and low processing cost.[17,18] It is of great significance to utilize the advantage of flow forming in the fabrication of thin-walled metal tubes to produce high-precision magnesium alloy tubes.

Park et al.[19] determined the magnitude of radial, axial, and tangential forces on the barrel during the flow-forming stage by analyzing the processing of the spun barrel and combining the flow functions. Chang et al.[20] focused on the effect of different forming passes on the organization and properties of aluminum alloy spun tubes. Katherine et al.[21] constructed a model by finite-element analysis software and verified the feasibility of the model with experiments. The influence of different flow-forming process parameters on the material forming properties was investigated. However, the research on the direct relationship between the microstructure evolution and the properties in the plastic deformation process of flow forming cylindrical parts mainly stays at the qualitative level through microstructure analysis, which does not give quantitative results.

*Corresponding author's e-mail:
wangwenxian@tyut.edu.cn (Wenxian Wang)

In this work, the microstructure evolution and nanomechanical behavior of magnesium alloy single-layer barrels under different thinning rates during flow forming were analyzed, and the load-displacement curve obtained by indentation was transformed into a stress-strain curve, which corresponded to the tensile experiment. It is found that controlling the thinning rate of the flow-forming process can effectively improve the mechanical properties of the magnesium alloy.

2 EXPERIMENTAL PART

An extruded AZ31B alloy was used to investigate the flow-forming process. The nominal composition of the AZ31B alloy is 0.04 *w*/% Cu, 1.0 *w*/% Zn, 0.8 *w*/% Mn, 2.5 *w*/% Al, 0.08 *w*/% Ca and balance Mg. Before flow forming, the billets were preheated to 623 K in an electrical furnace and the mandrel was preheated to the same temperature with electric heating pipes. The flow-forming process is shown in **Figure 1**. The spindle revolutions were 150 min^{-1}, the feed ratio was 1 mm/revolution and the thickness reduction was (0, 30 and 60) %, respectively. Following the flow forming, the specimens were cut parallel to the RD-AD plane (longitudinal section).

To obtain reliable nano-indentation data, the nano-indentation tester (Nano Indenter G200) micro- and nano-mechanical tester with standard XP system from Agilent was used to test the micro- and nano-mechanical behavior of different micro-zones of the Al alloy cylinder. For each specimen, indentation tests were performed with maximum loads of (20, 30, 40 and 50) mN, where the loading duration was 15 s. At least three indentation tests were performed at different maximum loads, while maintaining sufficient intervals between each indentation. The micro- and nano-mechanical properties of the characterized materials were further analyzed by nano-indentation experiments. A detailed microstructural analysis was performed by electron back-scattered diffraction (EBSD) on a TESCAN MIRA3 scanning electron microscope. The testing plane of the EBSD was RD*AD, and the measurement was taken at 20 kV with a 15-mm working distance, a tilt angle of 70°, and a scanning step of 1.5 µm. The tensile properties of the material along the AD were measured with a universal testing machine (SDS-100) at a rate of 1 mm/min, the measured length and width of the tensile specimens were 20 mm and 5 mm, respectively.

3 RESULTS AND DISCUSSION

Figure 2 shows the grain sizes of the AZ31B Mg alloys with (0, 30 and 60) % thinning, respectively. With an increase of the thinning rate, the average grain size of AZ31B Mg alloys changes from 10.040 µm to 2.423 µm, which is caused by large plastic deformation, and a large number of low-angle boundaries appear at the same time.

During thermal deformation, it is easy to obtain a strong texture, which has a great influence on the mechanical properties of magnesium alloys.[22] **Figure 3** shows the pole figures of blanks at thickness reductions of (0, 30 and 60) %, respectively. Through the evolution of the microstructure, it can be seen that the grains of the AZ31B Mg alloy in the initial state have a strong {0 0 0 1} basal texture. When the thinning rate is 30 %, a large number of {-1 2 -1 0} and {0 1 -1 0} textures ap-

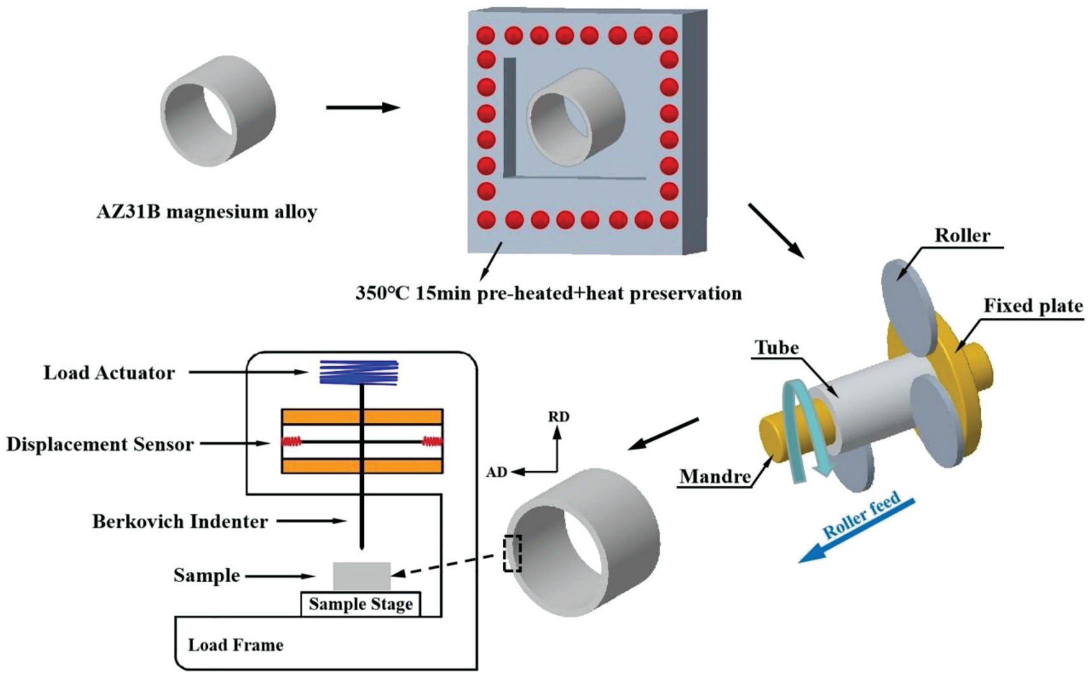

Figure 1: Schematic diagram of the whole experimental procedures

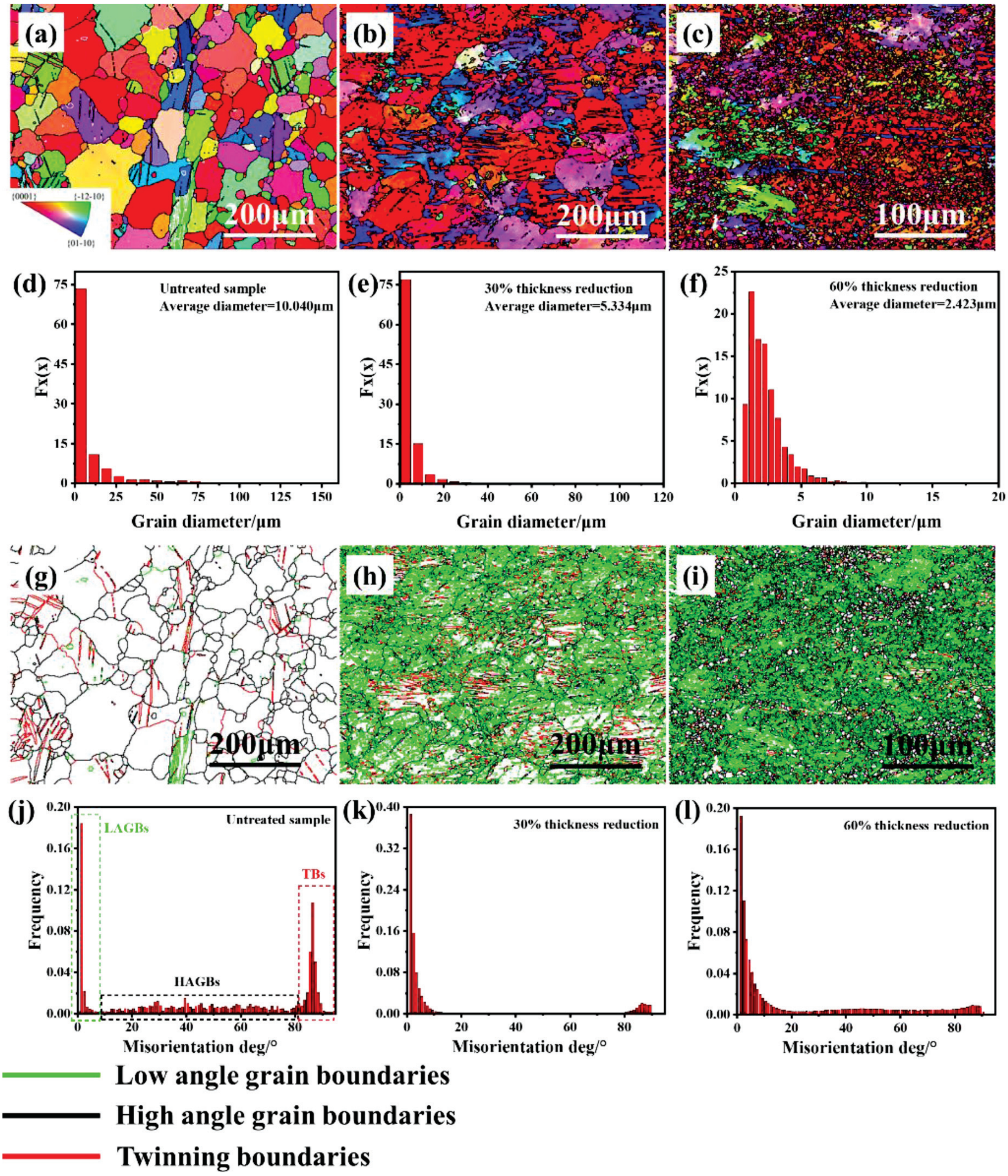

Figure 2: Microstructure evolution of flow-forming AZ31B Mg alloys

pear, and a large number of {-1 2 -1 0} tensile twins are produced. The results reveal that {-1 2 -1 0} tensile twins are dominant in the early deformation process. Twins are activated in most grains, but there are still some grains without twins. When the thinning rate continues to increase to 60 %, the texture type is consistent with that when the thinning rate is 30 %, and the number of {0 1 -1 0} stretching twins increases significantly, indicating that when the deformation is large, the {0 1 -1 0} stretching twins are gradually activated due to the presence of external forces.

From **Figure 4a** it can be observed that most of the grains of the base material on one side of the magnesium alloy are concentrated around the orientation factor of 0.4–0.5. The closer the Schmidt factor value in the figure is to 0.5, the color tends to be more red. The orientation factor is called soft orientation, which means that it is easier to trigger the opening of the slip system under the

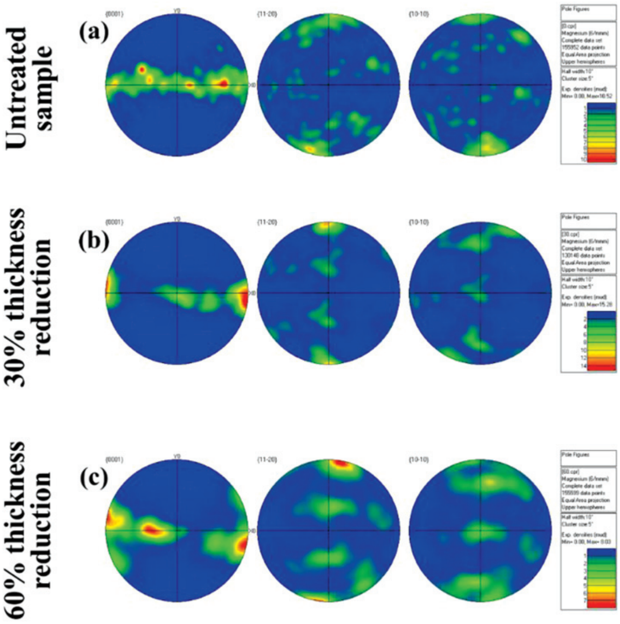

Figure 3: Pole figures of flow-forming AZ31B Mg at reduction rates: a) 0 %, b) 30 % and c) 60 %

action of external forces to occur the macroscopic plastic deformation. As the thinning rate increases to 30 %, the value of the Schmidt factor on one side of the magnesium alloy decreases significantly, and the proportion of the SF value less than 0.3 is about 95.7 %, and most of them are blue-green in **Figure 4b**, so it is difficult for the crystal to slip in the subsequent deformation. When the thinning rate increases to 60 %, the values of the orientation factor are more evenly distributed, but most of them are still concentrated below 0.3, as shown in **Figure 4c**. As the thinning rate increases from 30 % to 60 %, the crystals, which are not susceptible to slip, are deformed significantly, so the material changes its mechanism at larger deformations.

Dynamic recrystallization (DRX) has a significant role in the large strain thermal deformation of magnesium alloys.[23,24] Therefore, it is necessary to further investigate the behavior of DRX in hot-flow-forming processes. As observed in **Figure 5**, the base material of the barrel is mainly composed of about 93 % recrystallized grains and a small number of twins, indicating that dynamic recrystallization of the base material mainly occurs during the extrusion process due to large deformation. In addition, a small number of sub-crystals are distributed at the grain boundaries or twins of the recrystallized grains. With the increase of the thinning rate to 30 %, the barrel-shaped parts under the action of external forces undergo large plastic deformation, the interior of the magnesium alloy mainly consists of about 73 % of deformed grains and a small part of sub-crystals, where the twin crystals are mainly distributed in the deformed grains. In this flow-forming process, the magnesium alloy side by a large number of recrystallized grains in the base material after a large plastic deformation into deformed grains. As can be seen from **Figure 5b**, the magnesium alloy is more difficult to slip at the grain boundaries, the deformation is not large, but a large deformation occurs inside the grain, so the deformation of the whole grain is not uniform. As the thinning rate continues to increase to 60 %, the interior of the magnesium

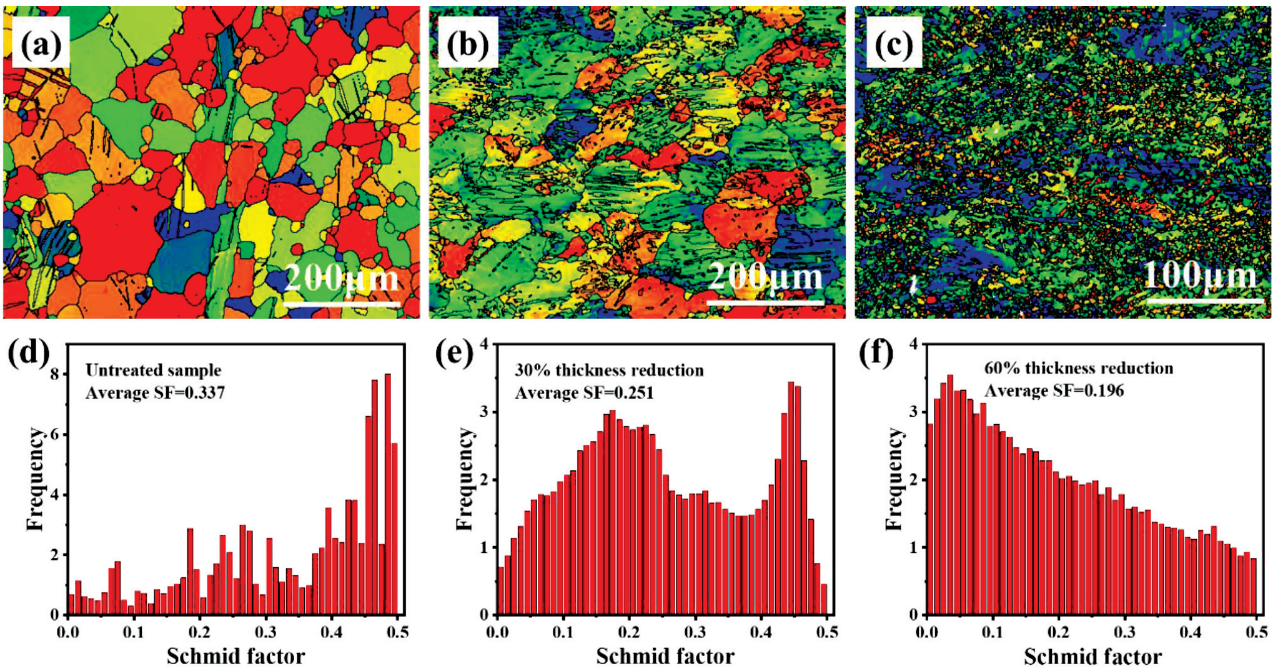

Figure 4: Schmid factor distribution on AZ31BMg under different thickness reductions after flow forming: a) and d) 0 %, b) and e) 30 %, c) and f) 60 %

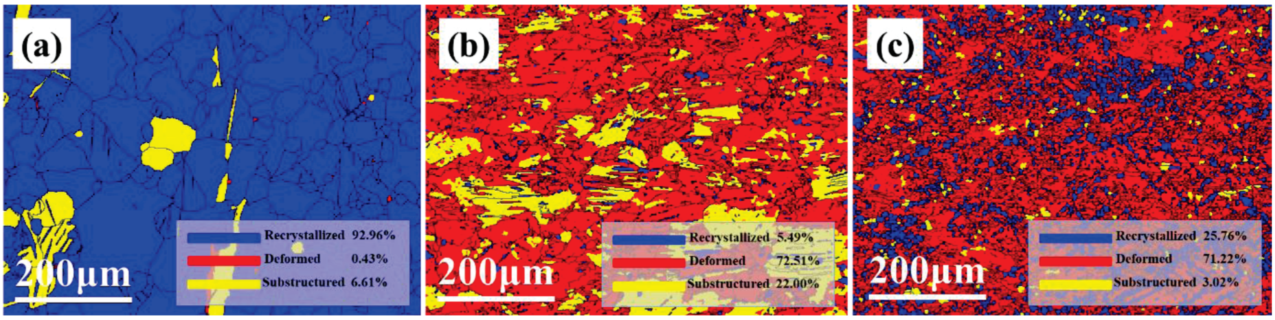

Figure 5: The distribution of recrystallized, deformed, and sub-structured grains of Mg under different thickness reductions after flow forming: a) 0 %; b) 30 %; c) 60 %

alloy side is mainly composed of about 71 % of deformed grains and about 26 % of recrystallized grains, where the number of twins is significantly reduced compared to the thinning rate of 30 %, and the grains undergo significant refinement mainly due to the action of twins driving dynamic recrystallization. **Figure 5c** illustrates that the sub-crystalline grains are basically transformed into recrystallized grains during the flow-forming process, which is due to the combined effect of the dominant twin drive within the sub-crystal and the dislocation plugging at the sub-crystal boundaries under large strain conditions. During the thermal flow forming process, the sub-crystal boundaries tend to migrate into large-angle grain boundaries due to the large dislocation difference around the sub-crystal boundaries, which are used as the nuclei for recrystallization and growth.

From the distribution of dislocations in **Figure 6**, it can be noted that the local orientation difference in the parent material is small, indicating that the dislocation density of the parent material on the side of magnesium alloy is relatively small. With the increase of the thinning rate, twin deformation occurs inside the magnesium alloy during the spinning process, then the two parts of deformed and undeformed crystals, i.e., twin crystals, will be constrained by the matrix and produce larger strain. Therefore, when the thinning rate reaches 60 %, the internal local orientation difference is relatively large. And the average KAM of the base material is calculated to be 4.003°, and when the thinning rate reaches 30 %, the size of the dislocation density inside the magnesium alloy increases significantly to 17.495°, and with the increase of the thinning rate the dislocation density inside the material remains almost constant at about 17.547°.

Figure 7a to **7c** show the load-displacement curves of AZ31B Mg alloys with different thinning rates (0, 30 and 60) % at different maximum loads (20, 30, 40 and

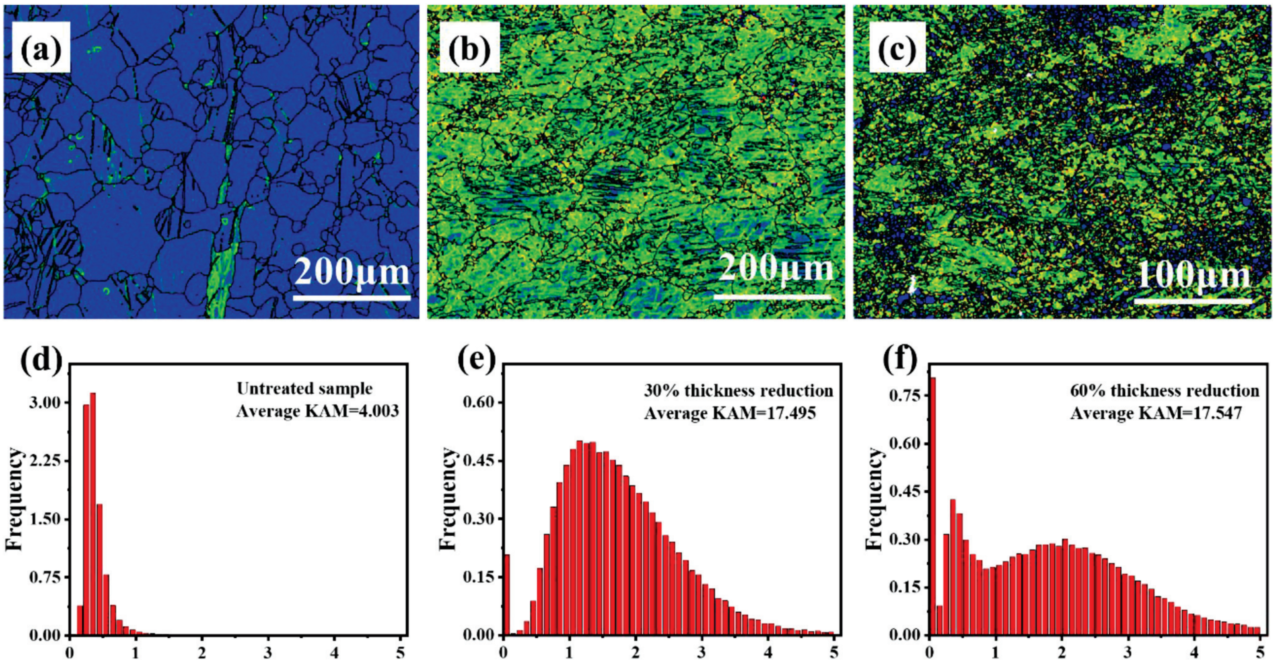

Figure 6: Different thickness reductions of flow forming: a) and d) 0%, b) and e) 30 %, c) and f) 60 %

50) mN. Overall, the loading phase curves of the load-displacement curves at different thinning rates almost overlap, which indicates that the indentation behavior of the flow-forming barrels is not sensitive to the loading rate. With the increase of the thinning rate, the maximum displacement depth gradually decreases, and its displacement depth decreases more obviously with the increase of the maximum indentation load. The stress-strain curves of the AZ31B magnesium alloy are presented in **Figure 7d** to **7f**. The elastic modulus of the barrel-shaped parts increased slightly from (50.3 ± 0.6) GPa to (51.9 ± 0.4) GPa with the increase of the thinning rate after flow forming, which is mainly due to the twinning deformation inside the grains during the flow-forming process, and the number and position of the twins have a greater influence on the elastic modulus obtained from the test. In addition, with the increase of the thinning rate, the yield strength σ_y of AZ31B magnesium alloy has a significant increase, and the indentation yield strength is (212.0 ± 0.5) MPa, after the thinning rate of 30 % and 60 % increased to (227.5 ± 0.8) MPa and (248.2 ± 0.5) MPa, respectively, and the elastic modulus increases from **Figure 7g**, **Figure 7h** and **Figure 7i** contains the graphs of the tensile tests, which provide strong evidence to verify the accuracy of the stress-strain data calculated from the nanoindentation.

4 CONCLUSIONS

The change of thinning rate during flow forming affects the relationship between the microstructure evolution and the mechanical properties of a magnesium alloy. The following main conclusions were drawn:

1) There is a significant grain refinement after hot flow forming. As the thickness decreases, the grain size decreases and the average value of hardness increases significantly.

2) This behavior is related to the microstructural evolution, which is strongly influenced by the depression

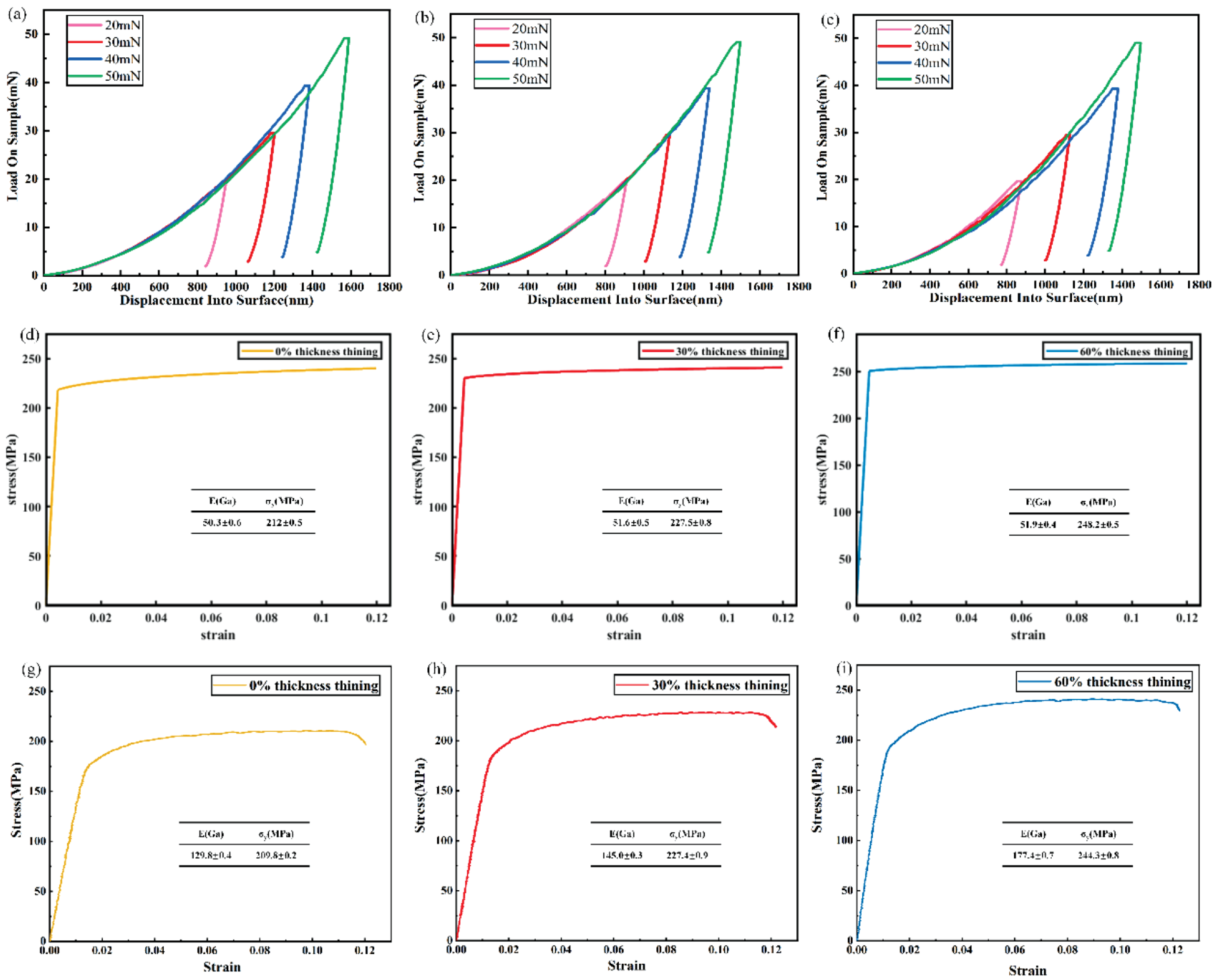

Figure 7: Typical load-displacement curves, stress-strain curves and tensile curves of Mg under different thickness reductions after flow forming: a), d) and g) 0 %; b), e) and h) 30 %; c), f) and i) 60 %

rate, due to the occurrence of grain-boundary sliding, dynamic recrystallization and grain growth.

3) High micro- and nano-mechanical properties are obtained when hot flow forming is performed at a temperature of 623 K, a spindle rotation of 150 min^{-1}, a feed ratio of 0.1 mm/revolution and a thickness reduction of 60 %. The modulus of elasticity and hardness reached (51.9 ± 0.4) GPa and (248.2 ± 0.5) MPa.

Acknowledgment

This work was supported by National Natural Science Foundation of China (Grant Nos. 52075360 and 51805359).

5 REFERENCES

[1] G. Faraji, M. M. Mashhadi, H. S. Kim, Microstructure inhomogeneity in ultra-fine grained bulk AZ91 produced by accumulative back extrusion (ABE), Mater. Sci. Eng. A, 528 (**2011**) 13–14, 4312–4317, doi:10.1016/j.msea.2011.02.075

[2] T. C. Xu, Y. Yang, X. D. Peng, J. F. Song, F. S. Pan, Overview of advancement and development trend on magnesium alloy, J. Magnes. Alloy., 7 (**2019**) 3, 536–544, doi:10.1016/j.jma.2019.08.001

[3] Y. Yang, X. M. Xiong, J. Chen, X. D. Peng, D. L. Chen, F. S. Pan, Research advances in magnesium and magnesium alloys worldwide in 2020, J. Magnes. Alloy., 9 (**2021**) 3, 705–747, doi:10.1016/j.jma.2021.04.001

[4] J. F. Song, J. Chen, X. M. Xiong, X. D. Peng, D. L. Chen, F. S. Pan, Research advances of magnesium and magnesium alloys worldwide in 2021, J. Magnes. Alloy., 10 (**2022**) 4, 863–898, doi:10.1016/j.jma.2022.04.001

[5] C. Bruni, A. Forcellese, F. Gabrielli, M. Simoncini, Effect of temperature, strain rate and fibre orientation on the plastic flow behaviour and formability of AZ31 magnesium alloy, J. Mater. Process. Technol., 210 (**2010**) 10, 1354–1363, doi:10.1016/j.jmatprotec.2010.03.025

[6] Z. R. Zeng, N. Stanford, C. H. J. Davies, J. F. Nie, B. Nick, Magnesium extrusion alloys: a review of developments and prospects, Int. Mater. Rev., 64 (**2019**) 1, 27–62, doi:10.1080/09506608.2017.1421439

[7] T. T. T. Trang, J. H. Zhang, J. H. Kim, A. Zargaran, J. H. Hwang, B. C. Suh, N. J. Kim, Designing a magnesium alloy with high strength and high formability, Nat. Commun., 9 (**2018**) 1, 1–6, doi:10.1038/s41467-018-04981-4

[8] A. Javaid, F. Czerwinski, Progress in twin roll casting of magnesium alloys: A review, J. Magnes. Alloy., 9 (**2020**) 2, 362–391, doi:10.1016/j.jma.2020.10.003

[9] H. Watari, T. Haga, N. Koga, K. Davey, Feasibility study of twin roll casting process for magnesium alloys, J. Mater. Process. Technol., 192 (**2007**), 300–305, doi:10.1016/j.jmatprotec.2007.04.009

[10] S. Y. Wang, L Gao, A. A. Luo, D. J. Li, X. Q. Zeng, Hot deformation behavior and workability of pre-extruded ZK60A magnesium alloy, Trans. Nonferrous Met. Soc. China, 25 (**2015**) 6, 1822–1830

[11] P. Peng, B. Wang, S. B. Zhou, J. She, A. T. Tang, J. Y. Zhang, F. S. Pan, Effects of optimizing continuous forging extrusion process on the microstructure and mechanical properties of AZ31 magnesium alloy, Mater. Sci. Eng. A, 840 (**2022**) 142892, doi:10.1016/j.msea.2022.142892

[12] Q. Xia, J. Long, G. Xiao, S. Yuan, Y. Qin, Deformation mechanism of ZK61 magnesium alloy cylindrical parts with longitudinal inner ribs during hot backward flow forming, Journal of Materials Processing Technology, 296 (**2021**), 117197, doi:10.1016/j.jmatprotec.2021.117197

[13] Z. Cao, F. Wang, Q. Wan, Z. Zhang, L. Jin, J. Dong, Microstructure and mechanical properties of AZ80 magnesium alloy tube fabricated by hot flow forming, Materials & Design, 67 (**2015**), 64–71, doi:10.1016/j.matdes.2014.11.016

[14] S. C. Chang, C. A. Huang, S. Y. Yu, Y. Chang, W. C. Han, T. S. Shieh, H. C. Chung, H. T. Yao, G. D. Shyu, H. Y. Hou, C. C. Wang, W. S. Wang, Tube spinnability of AA 2024 and 7075 aluminum alloys, J. Mater. Process. Technol., 80 (**1998**). 676–682, doi:10.1016/S0924-0136(98)00174-5

[15] K. M. Rajan, K. Narasimhan, An Investigation of the Development of Defects During Flow Forming of High Strength Thin Wall Steel Tubes, Pract. Fail. Anal., 1 (**2001**) 5, 69–76, doi:10.1007/BF02715366

[16] M. Haghshenas, M. Jhaver, R. J. Klassen, J. T. Wood, Plastic strain distribution during splined-mandrel flow forming, Mater. Des., 32 (**2011**) 6, 3629–3636, doi:10.1016/j.matdes.2011.02.014

[17] H. R. Molladavoudi, F. Djavanroodi, Experimental study of thickness reduction effects on mechanical properties and spinning accuracy of aluminum 7075-O, during flow forming, Int. J. Adv. Manuf. Technol., 52 (**2010**) 9–12, 949–957, doi:10.1007/s00170-010-2782-4

[18] H. Zoghi, A. F. Arezoodar, M. Sayeaftabi, Enhanced finite element analysis of material deformation and strain distribution in spinning of 42CrMo steel tubes at elevated temperature, Mater. Des., 47 (**2013**), 234–242, doi:10.1016/j.matdes.2012.11.049

[19] J. W. Park, Y. H. Kim, W. B. Bae, Analysis of tube-spinning processes by the upper-bound stream-function method, Journal of Materials Processing Technology, 66 (**1997**) 1–3, 195–203, doi:10.1016/S0924-0136(96)02519-8

[20] S. C. Chang, C. A. Huang, S. Y. Yu, Y Chang, W. C. Han, T. S. Shieh, H. C. Chung, H. T. Yao, G. D. Shyu, H. Y. Hou, C. C. Wang, W. S. Wang, Tube spin ability of AA 2024 and 7075 aluminum alloys, Journal of Materials Processing Technology, (1998), 80-81, 676–682, doi:10.1016/S0924-0136(98)00174-5

[21] M. O. Katherine, G. D. João, R. M. A. Conrado, J. M. Meza, J. U. Selgado, Experimental study and thermodynamic computational simulation of phase transformations in centrifugal casting bimetallic pipe of API 5L X65Q steel and Inconel 625 alloy, Journal of Manufacturing Processes, 32 (**2018**), 318–326, doi:10.1016/j.jmapro.2018.02.003

[22] W. J. Kim, S. I. Hong, Y. S. Kim, S. H. Min, H. T. Jeong, J. D. Lee, Texture development and its effect on mechanical properties of an AZ61 Mg alloy fabricated by equal channel angular pressing, J. Acta Materialia, 51 (**2003**) 11, 3293–3307, doi:10.1016/S1359-6454(03)00161-7

[23] W. P. Peng, P. J. Li, P. Zeng, L. P. Lei, Hot deformation behavior and microstructure evolution of twin-roll-cast Mg–2.9Al–0.9Zn alloy: a study with processing map, Mater. Sci. Eng. A, 494 (**2008**) 1–2, 173–178, doi:10.1016/j.msea.2008.04.029

[24] Z. Cao, F. Wang, Q. Wan, Z. Zhang, L. Jin, J. Dong, Microstructure and mechanical properties of AZ80 magnesium alloy tube fabricated by hot flow forming, Materials & Design, 67 (**2015**), 64–71, doi:10.1016/j.matdes.2014.11.016